Nuclear Materials and Energy 12 (2017) 918–923

Contents lists available at ScienceDirect

Nuclear Materials and Energy

journal homepage: www.elsevier.com/locate/nme

Assessment of X-point target divertor configuration for power handling and detachment front control

M.V. Umansky[a,*], M.E. Rensink[a], T.D. Rognlien[a], B. LaBombard[b], D. Brunner[b], J.L. Terry[b], D.G. Whyte[b]

[a] Lawrence Livermore National Lab, Livermore, CA 94550, USA
[b] MIT Plasma Science and Fusion Center, Cambridge, MA 02139, USA

ARTICLE INFO

Article history:
Received 14 July 2016
Revised 1 February 2017
Accepted 9 March 2017
Available online 3 April 2017

ABSTRACT

A study of long-legged tokamak divertor configurations is performed with the edge transport code UEDGE (Rognlien et al., J. Nucl. Mater. 196, 347, 1992). The model parameters are based on the ADX tokamak concept design (LaBombard et al., Nucl. Fusion 55, 053020, 2015). Several long-legged divertor configurations are considered, in particular the X-point target configuration proposed for ADX, and compared with a standard divertor. For otherwise identical conditions, a scan of the input power from the core plasma is performed. It is found that as the power is reduced to a threshold value, the plasma in the outer leg transitions to a fully detached state which defines the upper limit on the power for detached divertor operation. Reducing the power further results in the detachment front shifting upstream but remaining stable. At low power the detachment front eventually moves to the primary X-point, which is usually associated with degradation of the core plasma, and this defines the lower limit on the power for the detached divertor operation. For the studied parameters, the operation window for a detached divertor in the standard divertor configuration is very small, or even non-existent; under the same conditions for long-legged divertors the detached operation window is quite large, in particular for the X-point target configuration, allowing a factor of 5–10 variation in the input power. These modeling results point to possibility of stable fully detached divertor operation for a tokamak with extended divertor legs.

1. Introduction

A tokamak-based fusion reactor is expected to have extremely high power exhaust densities which would overwhelm existing tokamak divertor designs by causing very high heat flux densities leading to prohibitively high levels of material erosion from the plasma-facing components. This has motivated strong interest in innovative magnetic configurations. Some novel designs proposed in the recent years include divertors with radially extended divertor legs as in the super-X divertor [1]; using higher-order magnetic nulls as in the snowflake [2] and cloverleaf configurations [3]; using secondary X-points in the divertor volume or close to the target plate such as in the cusp divertor [4], X-divertor [5], and also in the inexact snowflake, i.e., snowflake-plus and snowflake-minus, configurations [2].

A recent idea is the X-point target divertor (XPTD) configuration [6] which combines the radially extended divertor leg like in super-X with a secondary X-point in the divertor volume. This arrangement may promote a stable, highly radiating detached plasma condition in the divertor leg, but located away from target plates [6].

Edge plasma transport codes such as UEDGE [7], SOLPS [8], and EDGE2D [9] are ideal tools to explore and evaluate innovative divertor configurations for potential performance enhancements. For UEDGE in particular, recent upgrades allowing inclusion of secondary X-points in the divertor extends the code's applicability to interesting magnetic topologies. Previous applications of edge transport codes to innovative divertors include [10–12]; however the recent upgrades to UEDGE increment the modeling capability by combining an advanced edge plasma physics model with detailed treatment of the divertor geometry.

In the study reported here, UEDGE is applied to three long-legged divertor configurations: X-point target divertor (XPTD), super-X divertor (SXD), and a long vertical leg divertor (LVLD);

* Corresponding author.
E-mail address: umansky1@llnl.gov (M.V. Umansky).

http://dx.doi.org/10.1016/j.nme.2017.03.015

and, for comparison, to a standard vertical plate divertor (SVPD) for parameters based on the ADX tokamak concept design [6]. The long-term goal of the study is to compare the responses of the various divertor configurations as power is varied and address some key questions such as: What is the maximum power level in which a detached divertor condition is obtained? What is the power level at which the detachment front starts to encroach on the main plasma? Can a stable detached divertor condition be maintained?

Although substantially more work will be needed to provide comprehensive answers, the results obtained so far point to the beneficial role of extended divertor leg geometry for entering and maintaining a stable detached divertor regime for a wide range of exhaust power.

2. Simulation setup

The four modeled cases are based on the geometry and parameters from ADX tokamak design. Starting from the same (or close) ADX MHD equilibria, the target plates are introduced at various locations to produce (i) X-point target divertor (XPTD), (ii) super-X divertor (SXD), (iii) long vertical leg divertor (LVLD), and (iv) standard vertical plate divertor (SVPD), see Fig. (1),

The SOL radial temperature and density profiles are set to match the ADX projections, based on the existing scalings. A radially growing profile for the density diffusing coefficient is used to match the expected mid-plane radial density profile width $\sim$ 5 mm; and a spatially constant $\chi_{e,i}$ is used to achieve $\sim$ 3 mm width of the mid-plane T_e profiles. Plasma density at the core interface is fixed at 1×10^{20} m^{-3}, and the resulting value at the separatrix is close to 0.5×10^{20} m^{-3}, see Fig. (2). This is at the low end of separatrix densities anticipated for ADX, representing the most challenging upstream conditions for divertor power handling.

Most of the runs use fully recycling wall boundary conditions on all material surfaces (unless stated otherwise), which is appropriate to simulate steady state reactor conditions. A fluid neutral model is employed. In all code runs a 1% carbon seed impurity is used, in the "fixed fraction" model [13]. Note that this impurity level, if fully ionized, would lead to Zeff=1.3. The geometry is assumed to be up-down symmetric and only the lower half-domain is modeled; the power into the lower half-domain, $P_{1/2}$ is used as a control parameter.

The standard UEDGE plasma model [14] is used in all runs reported here; however terms with plasma drifts and currents are not included to simplify the model. It is generally understood that the physics of divertor detachment is dominated by interplay of parallel plasma transport and atomic processes. Drifts and currents have an effect on detachment, as seen from B_t reversal divertor experiments [15,16], however the effect is quantitative rather than qualitative which probably justifies neglecting those terms for a first scoping study like this one. Treatment of neutrals in the runs reported here is dealt with by a fluid neutrals model [17] which is the standard option in UEDGE. Fluid treatment for neutrals is justified when the neutral atom charge-exchange (CX) mean-free-path is short compared to the neutral gas spatial scales of interest; the validity of this assumption should be verified aposteriori examining the numerical solutions.

3. Simulation results

Using the same physics model, and employing the cross-field transport coefficients shown in Fig. (2), a scan of the input power, $P_{1/2}$, is carried out for all four studied configurations. Observations are focused on the outer leg as the most challenging area in terms of the peak heat flux since for a symmetric double-null configuration strongly dominant power is exhausted through the low-field side [6]. In addition, experiments find that as plasma

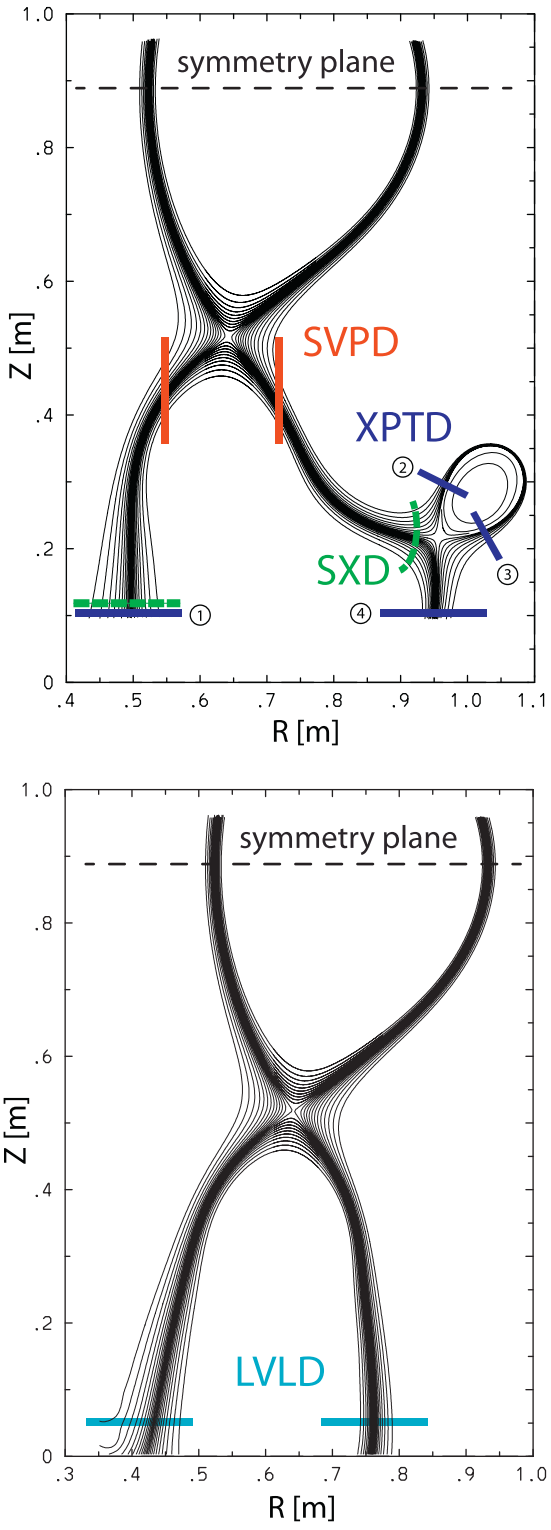

Fig. 1. UEDGE domain setup. Starting from the same (or close) ADX MHD equilibria, the target plates are introduced at various locations to produce (i) X-point target divertor (XPTD), (ii) super-X divertor (SXD), (iii) long vertical leg divertor (LVLD), and (iv) standard vertical plate divertor (SVPD). For XPTD the target plates are labeled according to the encircled numbers shown in the top diagram.

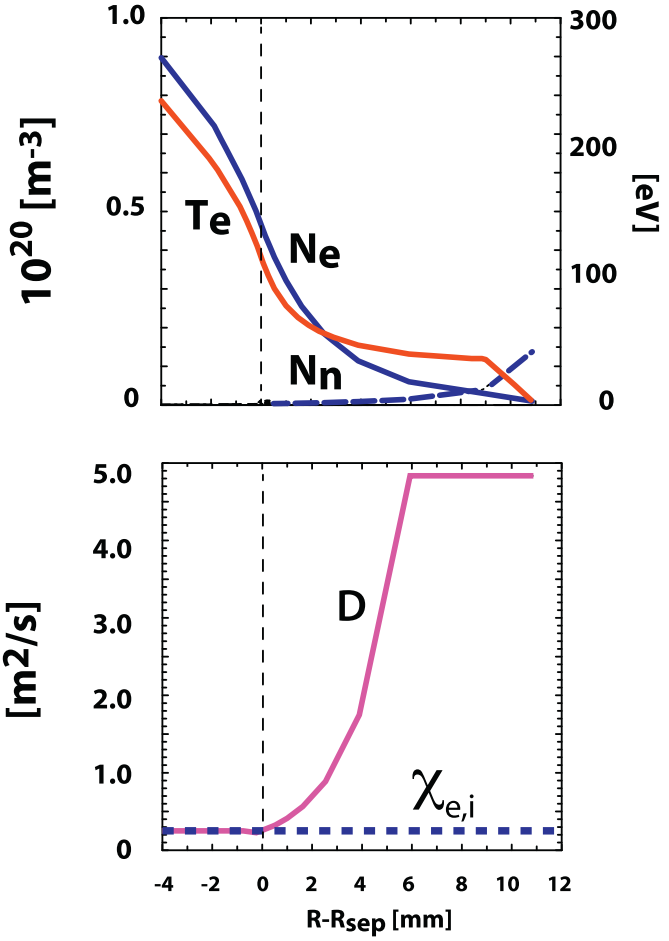

Fig. 2. Mid-plane plasma profiles for a representative XPTD case. Spatially constant $\chi_{e,i}$ and radially growing D are used to produce radial mid-plane plasma profiles matching the projections used for ADX. These same transport coefficients are used for all cases considered.

conditions are changed to access a detached divertor state (such as a ramp-up in density), the inner divertor detaches first, followed by the outer divertor [18,19]. The formation of an X-point MARFE occurs after the outer divertor achieves full detachment.

For the XPTD configuration, as the input power is reduced to a threshold value, the outer leg transitions to a fully detached state with the detachment front localized near the secondary X-point. Reducing the power further results in the front shifting upstream but remaining stable, see Fig. (3). At even lower power the detachment front moves all way to the primary X-point.

For the other long-legged configurations, the evolution phases are qualitatively the same as for XPTD: at a threshold level $P_{1/2,\,max}$ the outer leg enters the detached divertor state; then as $P_{1/2}$ is reduced the location of the radiation front shifts upstream, and eventually, at $P_{1/2,\,min}$, it reaches the main X-point location.

A radiation front localized near the main X-point is usually associated with a MARFE that leads to main plasma degradation in the experiment. This sets the lower limit on $P_{1/2}$ for detached operation in our model.

For the standard divertor configuration (SVPD) there is no clear separation between entering the detached state and transitioning to a MARFE-like X-point radiation state, so the parameter window for detached operation is small or even non-existent for the studied SVPD configuration; on the other hand for the studied long-legged configurations there is a rather large separation between $P_{1/2,\,min}$ and $P_{1/2,\,max}$, in other words, a stable fully detached state is maintained over a significant range of the input power $P_{1/2}$. This is illustrated by Fig. (4) showing the maximum temperature on the plates vs. $P_{1/2}$.

The peak temperature dropping to a small value $\sim$ 1 eV is an indication of divertor detachment, also confirmed by observations of plasma and neutral gas density distribution in the divertor. As Fig. (4) shows, radially or vertically extended outer leg is beneficial for detached operation.

The long vertical leg (LVLD) allows entering the detached state at the level of input power $P_{1/2}$ not significantly lower than that for the radially extended leg (SXD). Based on the flux-expansion arguments in Ref. ([20].) one would expect $\sim$ 30% reduction of the detachment power threshold for SXD compared to LVLD but what we actually see in the simulations is significantly less. This suggests that some physics other than the magnetic flux expansion, perhaps neutrals, can play a more dominant role in setting the detachment characteristics in tightly baffled, long-leg divertors.

Another interesting observation that can be made from Fig. (4) is that a secondary X-point in the outer leg (XPTD) can significantly extend the window of $P_{1/2}$ for detached divertor operation–about a factor of 2 enhancement over the SXD case in this study. The potential performance gains afforded by these advanced divertor geometries are very impressive and encouraging–a factor of 5 to 10 increase in power handling with a stable detached divertor condition maintained for over a factor of 5 to 10 variation in exhaust power.

4. Discussion

The basic concept of divertor plasma detached from material walls by a layer of neutral gas was proposed in mid-1970s [21], and the detached divertor regime was closely looked at in the early stages of ITER design [22]. Since then, however, the ensuing body of extensive experimental work on many tokamaks has shown that the stable location for the radiation front is near the primary X-point, which was confirmed by a range of analytical and computational modeling studies, see Ref. ([23]) and references therein.

However, the radiation front located near the main X-point (i.e., close to the H-mode pedestal) has a strong negative effect on the main plasma performance, according to experience in current experiments which often show that complete detachment leads to MARFE and usually to a subsequent plasma disruption in L-mode, or transition to L-mode for H-mode plasmas [18,24–29].

As a result, the fully detached regime is currently considered a risky option for tokamak operation; instead a “partially detached” divertor regime is sought which means that plasma only in some flux tubes is detached from the divertor plate but elsewhere it is not. For example the current plans for ITER operation assume partially detached divertor [30].

Although numerical solutions with fully detached divertor have been documented in the literature, such solutions are usually fragile, requiring careful choice of model parameters, and with a small change of parameters easily transitioning to either a MARFE-like state or an attached state. For example the fully-detached state in UEDGE simulations in [31] transitions to a MARFE-like state as the input power is reduced by $\sim$ 50%. The fully detached state in another study with UEDGE [32] turns to attached with a relatively small tilting of the target plate. Simulations with EDGE2D-EIRENE and SOLPS for unstream density ramp in JET in [33] show that increasing the ustream density by some 10% beyond the detachment onset results in divertor plasma collapse associated with a massive penetration of neutrals to the core which would likely lead to a disruption in the experiment. SOLPS modeling in [34] shows that full detachment regime is correlated with strongly localized radiation in the proximity of the X- point and is prone to a radiation collapse of the plasma in the simulations.

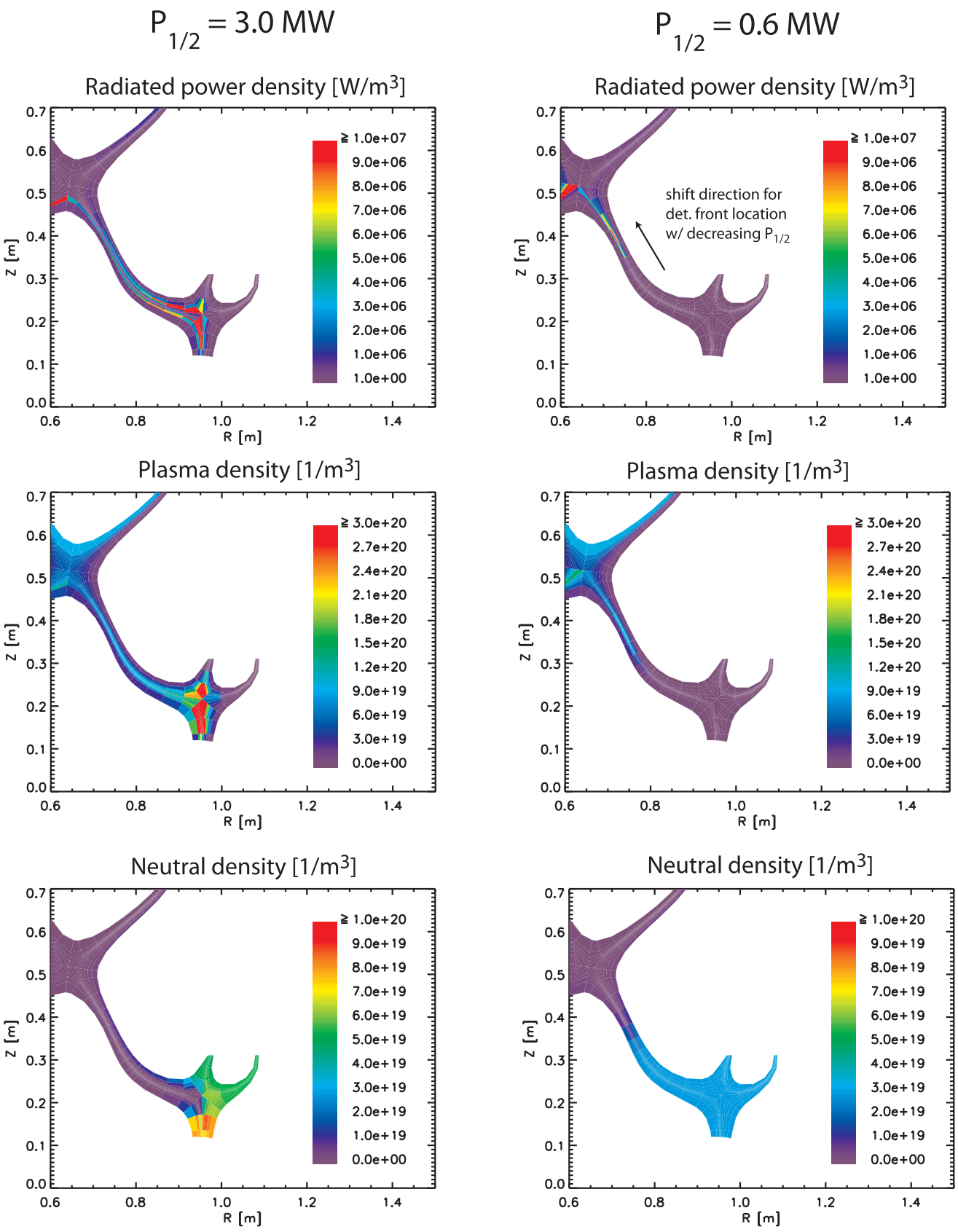

Fig. 3. Evolution of the detachment front for XPTD configuration. As the input power $P_{1/2}$ is reduced to a threshold value, the outer leg transitions to a fully detached state with the detachment front localized near the secondary X-point. Reducing the power further results in the front steady-state location shifting upstream while the leg volume below the radiation front fills up with neutral gas. Impurity radiation emissivity, plasma density, and neutral density is shown. The left column shows results for $P_{1/2}$=3.0 MW, slightly below the threshold level where detachment starts. The right column shows results for $P_{1/2}$=0.6 MW when the detachment front is not far from the main X-point.

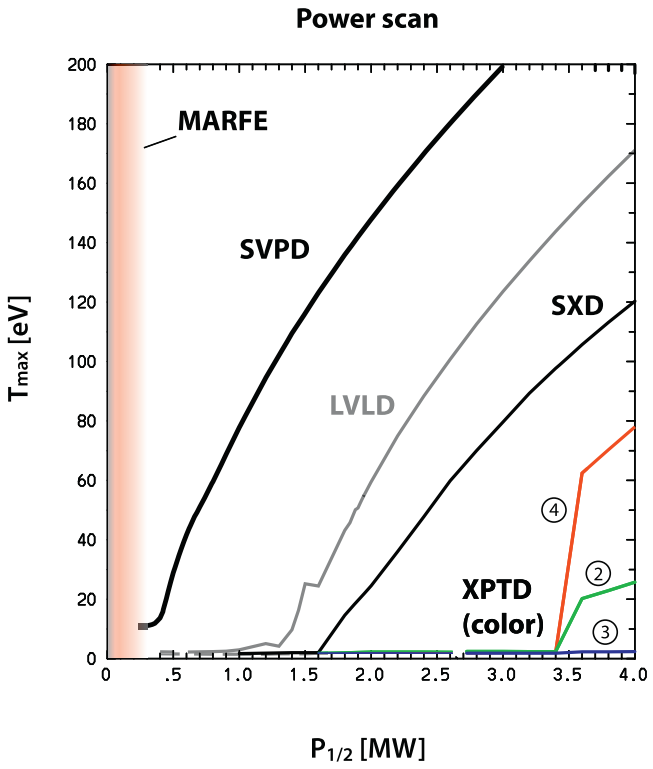

Fig. 4. The peak value of electron temperature on the outer divertor target T_{max} is plotted vs. the input power $P_{1/2}$. Traces for the peak electron temperatures at the three outer divertor targets for the XPTD configuration are shown in color and labeled according to the plate number, 2, 3 and 4, as shown in Fig. (1). As the input power is reduced the peak temperature drops to a small value, on the order of 1 eV which is a signature of entering a detached state. As the input power is reduced further the detachment front steady-state location shifts upstream. The detachment front localized near the main X-point is considered a MARFE-like state which defines the lower limit for the input power on the detached divertor operation window.

Contrary to the large body of modeling work described in the literature [31–34], the results presented here provide an example of the detached divertor state that persists for a rather broad range of parameters, as was intended in the original gas-box divertor concepts. There are indications that good confinement of neutral gas in the divertor channel is key for maintaining the fully-detached regime in the studied long-legged configurations; allowing for some wall pumping forces the detached plasma become attached to the divertor plate. The physics of these numerical solutions is still being investigated and detailed analysis will be deferred to a future publication.

One should note that for UEDGE solutions reported here plasma density in the divertor is $\geq 10^{20}\mathrm{m}^{-3}$ and temperature in the detached region is on the order of a few eV which leads to the neutral CX mean-free-path on the order of 1 cm or smaller. On the other hand, the perpendicular scale of neutral density across the divertor leg is on the order of 1 cm as well. Thus one should not expect the fluid neutrals model to be very accurate here; it is probably sufficient for a first scoping study but further investigation should aim to use more detailed models for the neutral gas. Similarly, using more detailed models of impurity ions and including plasma currents and drifts should be considered for further studies to address sensitivity of the results to details of the simulation model.

5. Conclusions

UEDGE is applied to three long-legged divertor configurations: X-point target divertor (XPTD), super-X divertor (SXD), and a long vertical leg divertor (LVLD); and, for comparison, to a standard vertical plate divertor (SVPD) for parameters based on the ADX tokamak concept design. The studied long-legged configurations are found to be strongly advantageous, compared to the standard divertor (SVPD), for entering and maintaining the detached divertor plasma state. Furthermore, a secondary X-point near to the end of a long outer divertor leg (XPTD) significantly extends the detached divertor operational window. A factor of 5 to 10 enhancement in the peak power handling and operational power window over a standard divertor is found in the present study. Overall, these results suggest feasibility of stable fully detached divertor operation for tokamaks with tightly baffled extended divertor legs.

Acknowledgment

Work performed for U.S. DOE by LLNL under Contract DE-AC52-07NA27344. The authors are grateful to Prof. B. Lipschultz for discussions of the 1-D model of detachment front in [20].

References

[1] P. Valanju, Super-X divertors and high power density fusion devices, Phys. Plas. 70 (2009) 056110.
[2] D.D. Ryutov, Geometrical properties of a snowflake divertor, Phys. Plasmas 14 (2007) 064502.
[3] D.D. Ryutov, M.V. Umansky, Divertor with a third-order null of the poloidal field, Phys. Plasmas 20 (2013) 092509.
[4] H. Takase, Guidance of divertor channel by cusp-like magnetic field for tokamak devices, J. Phys. Soc. Jpn. 70 (2001) 609.
[5] M. Kotschenreuther, Scrape off layer physics for burning plasmas and innovative divertor solutions, in: Proc. 20nd IAEA Fusion Energy Conference, IAEA, Vilamoura, Portugal, 2004. CD-ROM file IC/P6-43
[6] B. LaBombard, ADX: A high field, high power density, advanced divertor and RF tokamak, Nucl. Fus. 55 (2015) 053020.
[7] T. Rognlien, J. Milovich, M. Rensink, G. Porter, A fully implicit, time-dependent 2-D fluid code for modeling tokamak edge plasmas, J. Nuc. Mat. 196 (1992). 347–123
[8] R. Schneider, D. Reiter, H.P. Zehrfeld, B. Braams, M. Baelmans, B2-EIRENE simulation of ASDEX and ASDEX-Upgrade scrape-off layer plasmas, J. Nuc. Mat. 196–198 (1992) 810.
[9] R. Simonini, G. Corrigan, G. Radford, J. Spence, A. Taroni, Models and numerics in the multi-fluid 2-D edge plasma code EDGE-2D/U, Contrib. Plasma Phys. 34 (2–3) (1994) 368–373, doi:10.1002/ctpp.2150340242.
[10] T. Lunt, G. Canal, B.P. Duval, Y. Feng, B. Labit, P. McCarthy, H. Reimerdes, W.A.J. Vijvers, M. Wischmeier, Numerical study of potential heat flux mitigation effects in the TCV snowflake divertor, Plasma Phys. Control. Fus. 58 (2016) 045027, doi:10.1088/0741-3335/58/4/045027.
[11] V.P. Ridolfini, R. Zagrski, G. Artaserse, G. Calabr, F. Crisanti, G. Maddaluno, G. Ramogida, B. Viola, Preliminary 2d code simulation of the quasi-snowflake divertor configuration in the FAST tokamak, Fus. Eng. Des. 88 (910) (2013) 1677–1681. Proceedings of the 27th Symposium On Fusion Technology (SOFT-27); Liége, Belgium, September 24–28, 2012. http://dx.doi.org/10.1016/j.fusengdes.2013.05.093 URL http://www.sciencedirect.com/science/article/pii/S0920379613005334.
[12] M.V. Umansky, R.H. Bulmer, R.H. Cohen, T.D. Rognlien, D.D. Ryutov, Analysis of geometric variations in high-power tokamak divertors, Nucl. Fus. 49 (2009) 075005.
[13] R.A. Hulse, Numerical studies of impurities in fusion plasmas, Nucl. Technol. Fus. 3 (1983) 259.
[14] T.D. Rognlien, D.D. Ryutov, N. Mattor, G.D. Porter, Two-dimensional electric fields and drifts near the magnetic separatrix in divertor tokamaks, Phys. Plasmas 6 (5) (1999) 1851–1857, doi:10.1063/1.873488.
[15] I.H. Hutchinson, B. LaBombard, J.A. Goetz, B. Lipschultz, G.M. McCracken, J.A. Snipes, J.L. Terry, The effects of field reversal on the Alcator C-Mod divertor, Plasma Phys. Control. Fus. 37 (12) (1995) 1389. URL http://stacks.iop.org/0741-3335/37/i=12/a=004.
[16] A.G. McLean, Drift-driven divertor asymmetries in the transition from attached to fully detached conditions, Paper Presented at the Meeting of American Physical Society, Division of Plasma Physics, Savannah, Georgia, 2015.
[17] F. Wising, D.A. Knoll, S.I. Krasheninnikov, T.D. Rognlien, D.J. Sigmar, Simulation of the Alcator C-Mod divertor with an improved neutral fluid model, Contrib. Plasma Phys. 36 (2–3) (1996) 136–139, doi:10.1002/ctpp.2150360208.
[18] B. Lipschultz, B. LaBombard, J. Terry, C. Boswell, I. Hutchinson, Divertor physics research on Alcator C-Mod, Fus. Sci. Technol. 51 (3) (2007) 369–389.
[19] S. Potzel, M. Wischmeier, M. Bernert, R. Dux, H. Mller, A. Scarabosio, the ASDEX Upgrade Team, A new experimental classification of divertor detachment in ASDEX Upgrade, Nucl. Fus. 54 (1) (2014) 013001. URL http://stacks.iop.org/0029-5515/54/i=1/a=013001.
[20] B. Lipschultz, F.I. Parra, I.H. Hutchinson, Sensitivity of detachment extent to magnetic configuration and external parameters, Nucl. Fus. 56 (2016) 056007.

[21] F.H. Tenney, G. Lewin, A fusion power plant, Tech. Rep. MAT 1050, 1974.
[22] P.-H. Rebut, D. Boucher, D.J. Gambier, B.E. Keen, M.L. Watkins, The ITER challenge, Fus. Eng. Des. 22 (1993) 7–18.
[23] G. Matthews, Plasma detachment from divertor targets and limiters, J. Nucl. Mater. 220–222 (1995) 104–116.
[24] A. Loarte, R. Monk, J. Martn-Sols, D. Campbell, A. Chankin, S. Clement, S. Davies, J. Ehrenberg, S. Erents, H. Guo, P. Harbour, L. Horton, L. Ingesson, H. Jckel, J. Lingertat, C. Lowry, C. Maggi, G. Matthews, K. McCormick, D. O'Brien, R. Reichle, G. Saibene, R. Smith, M. Stamp, D. Stork, G. Vlases, Plasma detachment in JET Mark I divertor experiments, Nucl. Fus. 38 (3) (1998) 331. URL http://stacks.iop.org/0029-5515/38/i=3/a=303.
[25] M.E. Fenstermacher, J. Boedo, R.C. Isler, A.W. Leonard, G.D. Porter, D.G. Whyte, R.D. Wood, S.L. Allen, N.H. Brooks, R. Colchin, T.E. Evans, D.N. Hill, C.J. Lasnier, R.D. Lehmer, M.A. Mahdavi, R. Maingi, R.A. Moyer, T.W. Petrie, T.D. Rognlien, M.J. Schaffer, R.D. Stambaugh, M.R. Wade, J.G. Watkins, W.P. West, N. Wolf, Physics of the detached radiative divertor regime in DIII-D, Plasma Phys. Control. Fus. 41 (3A) (1999) A345. URL http://stacks.iop.org/0741-3335/41/i=3A/a=028.
[26] R. Pitts, B. Duval, A. Loarte, J.-M. Moret, J. Boedo, D. Coster, I. Furno, J. Horacek, A. Kukushkin, D. Reiter, J. Rommers, Divertor geometry effects on detachment in {TCV}, J. Nucl. Mater. 290–293 (2001) 940–946. 14th Int. Conf. on Plasma-Surface Interactions in Controlled Fusion Devices. http://dx.doi.org/10.1016/S0022-3115(00)00461-X. URL http://www.sciencedirect.com/science/article/pii/S002231150000461X.
[27] A. Kallenbach, M. Bernert, M. Beurskens, L. Casali, M. Dunne, T. Eich, L. Giannone, A. Herrmann, M. Maraschek, S. Potzel, F. Reimold, V. Rohde, J. Schweinzer, E. Viezzer, M. Wischmeier, the ASDEX Upgrade Team, Partial detachment of high power discharges in ASDEX Upgrade, Nucl. Fus. 55 (5) (2015) 053026. URL http://stacks.iop.org/0029-5515/55/i=5/a=053026.
[28] N. Asakura, N. Hosogane, K. Itami, A. Sakasai, S. Sakurai, K. Shimizu, M. Shimada, H. Kubo, S. Higashijma, H. Takenaga, H. Tamai, S. Konoshima, T. Sugie, K. Masaki, Y. Koide, O. Naito, H. Shirai, T. Takizuka, T. Ishijima, S. Suzuki, A. Kumagai, Role of divertor geometry on detachment and core plasma performance in {JT60u}, J. Nucl. Mater. 266–269 (1999) 182–188. http://dx.doi.org/10.1016/S0022-3115(98)00818-6. URL http://www.sciencedirect.com/science/article/pii/S0022311598008186.
[29] F. Reimold, M. Wischmeier, M. Bernert, S. Potzel, A. Kallenbach, H. Mller, B. Sieglin, U. Stroth, the ASDEX Upgrade Team, Divertor studies in nitrogen induced completely detached H-modes in full tungsten ASDEX Upgrade, Nucl. Fus. 55 (3) (2015) 033004. URL http://stacks.iop.org/0029-5515/55/i=3/a=033004.
[30] R.A. Pitts, Status and physics basis of the ITER divertor, Physica Scripta T138 (2009) 014001.
[31] R.E. Nygren, D.F. Cowgill, M.A. Ulrickson, B.E. Nelson, P.J. Fogarty, T. Rognlien, M.E. Rensink, A. Hassanein, S.S. Smolentsev, M. Kotschenreuther, Design integration of liquid surface divertors, Fus. Eng. Des. 72 (2004) 223.
[32] M.E. Rensink, T.D. Rognlien, Plasma heat-flux dispersal for ACT1 divertor, Fus. Sci. Technol. 67 (2015) 125.
[33] C. Guillemaut, R. Pitts, A. Kukushkin, J. Gunn, J. Bucalossi, G. Arnoux, P. Belo, S. Brezinsek, M. Brix, G. Corrigan, S. Devaux, J. Flanagan, M. Groth, D. Harting, A. Huber, S. Jachmich, U. Kruezi, M. Lehnen, C. Marchetto, S. Marsen, A. Meigs, O. Meyer, M. Stamp, J. Strachan, S. Wiesen, M. Wischmeier, J.E. Contributors, Influence of atomic physics on EDGE2D-EIRENE simulations of JET divertor detachment with carbon and beryllium/tungsten plasma-facing components, Nucl. Fus. 54 (9) (2014) 093012. URL http://stacks.iop.org/0029-5515/54/i=9/a=093012.
[34] F. Reimold, M. Wischmeier, M. Bernert, S. Potzel, D. Coster, X. Bonnin, D. Reiter, G. Meisl, A. Kallenbach, L. Aho-Mantila, U. Stroth, Experimental studies and modeling of complete h-mode divertor detachment in ASDEX Upgrade, J. Nucl. Mater. 463 (2015) 128–134. Proceedings of the 21st International Conference on Plasma-Surface Interactions in Controlled Fusion Devices Kanazawa, Japan May 26–30, 2014. http://dx.doi.org/10.1016/j.jnucmat.2014.12.019URL http://www.sciencedirect.com/science/article/pii/S002231151400960X.